Melatonin alleviates mitochondrial damage by regulating SIRT3-mediated mitochondrial dynamics in granulosa cells under PCOS-like conditions

CONGCONG XIE[1,2*], ZEHAO LIU[3*], TONG CHEN[4], HUI LU[2], XIUJIA ZHANG[2], WENBO YU[2], JIAXIN ZHANG[2], DANDAN SHANG[4] and XUEYING WANG[2]

[1]School of Physical Education, Shaanxi Normal University, Xi'an, Shanxi 710119, P.R. China; [2]Hebei Key Laboratory of Reproductive Medicine, Hebei Reproductive Health Hospital, Shijiazhuang, Hebei 050071, P.R. China; [3]Institute of Paediatrics, Hebei Provincial Clinical Research Centre for Child Health and Disease, Hebei Children's Hospital, Shijiazhuang, Hebei 050031, P.R. China; [4]Department of Biochemistry and Molecule Biology, Hebei Medical University, Shijiazhuang, Hebei 050017, P.R. China

Received October 8, 2025; Accepted May 22, 2026

DOI: 10.3892/mmr.2026.13937

Abstract. The present study investigated the role of melatonin (MT) in regulating mitochondrial function via sirtuin 3 (SIRT3) in granulosa cells (GCs) from patients with polycystic ovary syndrome (PCOS), with a focus on mitochondrial protection. Notably, GCs isolated from patients with PCOS exhibited mitochondrial dysfunction. Using an *in vitro* PCOS model established by treating KGN cells with dihydrotestosterone (DHT), decreased SIRT3 expression, dysregulated mitochondrial dynamics and hyperactivation of mitophagy were observed. Both SIRT3 overexpression and MT treatment restored the mitochondrial membrane potential, rebalanced mitochondrial dynamics and suppressed excessive autophagy in DHT-treated cells. Additionally, MT levels were shown to be reduced in the follicular fluid of patients with PCOS. Notably, the protective effects of MT on proteins associated with both mitochondrial dynamics and autophagy were abolished upon SIRT3 inhibition. In conclusion, mitochondrial dysfunction and aberrant mitophagy in GCs may serve a role in the pathogenesis of PCOS. MT appears to ameliorate these defects by modulating mitochondrial dynamics and function in a SIRT3-dependent manner. Moreover, the current study identified SIRT3 as a key molecular target of MT in PCOS.

Correspondence to: Dr Xueying Wang, Hebei Key Laboratory of Reproductive Medicine, Hebei Reproductive Health Hospital, 480 Heping Road, Xinhua, Shijiazhuang, Hebei 050071, P.R. China
E-mail: xuehuajingying@163.com

Dr Dandan Shang, Department of Biochemistry and Molecule Biology, Hebei Medical University, 361 Zhongshan Road, Chang'an, Shijiazhuang, Hebei 050017, P.R. China
E-mail: lily.dandan@163.com

*Contributed equally

Key words: polycystic ovary syndrome, mitochondrial function, sirtuin 3, melatonin

Introduction

Polycystic ovary syndrome (PCOS) is a prevalent endocrine disorder affecting 10-13% of women worldwide (1). PCOS is clinically defined by ovulatory dysfunction, hyperandrogenism, polycystic ovarian morphology and chronic inflammation (2). Notably, PCOS is associated with suboptimal pregnancy outcomes, primarily attributed to compromised oocyte quality, oxidative stress and mitochondrial dysfunction, with oocyte quality being a critical determinant of female fertility. Granulosa cells (GCs), key somatic support cells for oocytes, rely on functionally intact mitochondria to support their growth, proliferation and steroidogenic capacity (3). Mitochondrial dysfunction in GCs has emerged as a pivotal contributor to impaired oocyte maturation and reduced developmental competence in patients with PCOS (4,5). Studies have shown that in patients with PCOS, GCs exhibit decreased mitochondrial membrane potential (MMP) and impaired oxidative phosphorylation; these abnormalities lead to decreased ATP synthesis and antioxidant enzyme activity, and oxidative stress (6,7).

Research has shown that GCs from patients with PCOS exhibit reduced mitochondrial biosynthesis, aberrant fission and fusion dynamics, decreased MMP and activated mitochondrial autophagy (8). Mitochondrial fragmentation, resulting from imbalanced fission and fusion processes, is considered a prerequisite for the initiation of mitophagy (9,10). Notably, dynamin-related protein 1 (DRP1) serves a key role in mitochondrial dynamics; DRP1 mediates mitochondrial fission by interacting with mitochondrial outer membrane adaptor proteins, such as mitochondrial fission 1 protein (FIS1) and mitochondrial fission factor (11). These interactions lead to the formation of a division ring, which drives the fission process. Dysregulation of mitochondrial dynamics and abnormalities in the mitophagy pathway have been implicated in the pathogenesis of various diseases, including cardiovascular

disorders, cancer and neurodegenerative conditions (12-14). The sirtuin (SIRT) family comprises conserved class III histone deacetylases. Among them, SIRT3 is primarily localized to the mitochondria and has a pivotal role in preserving mitochondrial function (15). Bugga *et al* (16) revealed that SIRT3 may alleviate cardiac mitochondrial dysfunction by activating AMP-activated protein kinase (AMPK)/peroxisome proliferator-activated receptor γ coactivator (PGC)-1α signalling. SIRT3 knockdown impaired mitochondrial biogenesis and dynamics, whereas its overexpression upregulated the expression of mitochondrial DNA-encoded genes, increased superoxide dismutase 2 (SOD2) activity and altered mitochondrial dynamics. Additionally, SIRT3 overexpression increased the expression of mitochondrial biogenesis-related genes and proteins (PGC-1α and TFAM) (16). However, to the best of our knowledge, the role of SIRT3 in regulating mitochondrial dynamics in the GCs of patients with PCOS has not been reported. Therefore, investigating regulators of mitochondrial dynamics may offer insights for the development of novel therapeutic strategies for treating PCOS.

Melatonin (MT), a pineal hormone and potent antioxidant, regulates circadian rhythms and scavenges free radicals (17). The level of MT is greater in follicular fluid (FF) than in serum and it is markedly increased during follicular maturation. Notably, low levels of MT have been observed in the FF of patients with PCOS (18). Liu *et al* (19) reported that MT ameliorated cerebral ischaemia/reperfusion injury through the activation of SIRT3 signalling. Similarly, Wu *et al* (20) demonstrated that MT inhibited excessive mitochondrial autophagy in H9c2 cells through the MT membrane receptor 2 (MT2)/SIRT3/FoxO3a axis, thereby alleviating hypoxia/reoxygenation injury. However, the underlying molecular mechanism of MT in PCOS remains to be elucidated.

On the basis of accumulating evidence that mitochondrial dysfunction serves a pivotal role in PCOS pathogenesis and that SIRT3 acts as a key regulator of mitochondrial homeostasis, it was hypothesized that SIRT3-mediated disruption of mitochondrial dynamics in GCs could contribute to the development of PCOS, and that MT may ameliorate this dysfunction by upregulating SIRT3 expression. Specifically, the present study aimed to investigate the following: i) Whether GCs derived from patients with PCOS exhibit SIRT3 downregulation and aberrant mitochondrial dynamics; ii) whether SIRT3 overexpression can rescue mitochondrial function in a PCOS-like cellular model; iii) whether MT treatment can mimic the effects of SIRT3 overexpression; and iv) whether the protective effects of MT are dependent on SIRT3. Elucidation of these mechanisms may advance clinical diagnostics, treatment paradigms and assisted reproductive outcomes in patients with PCOS.

Materials and methods

Patients. Women who attended and were treated at the Reproductive Medicine Centre of Hebei Reproductive Health Hospital (Shijiazhuang, China) between June 2021 and June 2024 were included in the present study. Patients with PCOS (n=36) were diagnosed according to the Rotterdam criteria (21), and at least two of the following features were detected: Oligo-ovulation/anovulation, biochemical or clinical hyperandrogenism, and polycystic ovarian morphology on ultrasound. The exclusion criteria for the control and PCOS groups included the following: i) Ovarian cysts; ii) diminished ovarian reserve; iii) endometriosis; iv) hydrosalpinx; v) chromosomal abnormalities; or vi) chronic systemic conditions that could influence gene expression in GCs. The control group (n=41) included age-matched women with tubal factor infertility or who were undergoing fertility treatment due to male factor infertility, and with no endocrine abnormalities.

Isolation of cumulus GCs. Oocyte-cumulus complexes were retrieved by transvaginal ultrasound-guided follicular aspiration 36 h after human chorionic gonadotropin administration. The FF was collected from the same follicular aspirates after removal of the oocyte-cumulus complexes. Oocyte-cumulus complexes were subsequently washed in several flat dishes with G-Mopse PLUS (Vitrolife AB) to remove residual mural GCs, haemocytes and cellular debris. Cumulus complexes were identified under a microscope and mechanically flattened in Petri dishes. Cumulus GCs (CGCs) surrounding the oocytes were then carefully dissected.

Transmission electron microscopy (TEM). Following centrifugation at 400 x g for 10 min at room temperature, the CGCs were processed using standard ultrastructural techniques. The samples were fixed in 2.5% glutaraldehyde at 4˚C for 2 h and pre-embedded in 1% agarose (Ted Pella Inc.) to stabilize the pellet. Secondary fixation was performed with 1% osmium tetroxide for 2 h at room temperature, followed by sequential dehydration in a graded ethanol series. The specimens were then infiltrated and embedded in Araldite® epoxy resin. For TEM analysis, CGC samples from three randomly selected patients per group were examined. Ultrathin sections (60 nm) were prepared and allowed to air-dry overnight at room temperature. For staining, the sections were double-stained with 2% uranyl acetate in saturated alcoholic solution and lead citrate, each for 15 min at room temperature. Multiple ultrathin sections were prepared from each sample, and imaging areas were randomly selected at low magnification by electron microscopy technicians who were blinded to group allocation. Representative images were subsequently captured at higher magnifications to observe mitochondrial morphology and autophagic structures. A total of 10-15 cells were randomly selected from each sample. Autophagosomes were counted at the same magnification, and the results are presented as the mean ± SD for each group.

Cell culture. The human GC line KGN (cat. no. CL-0603), derived from a GC tumour, was obtained from Procell Life Science & Technology Co., Ltd. Both CGCs and KGN cells were maintained in DMEM/F-12 (cat. no. D6421; Sigma-Aldrich; Merck KGaA) supplemented with 10% heat-inactivated foetal bovine serum (FBS; cat. no. A5256701; Gibco; Thermo Fisher Scientific, Inc.) and 1% penicillin-streptomycin under standard culture conditions (37˚C, 5% CO_2). Cellular morphology and proliferation kinetics were monitored daily using phase contrast microscopy. At 80-90% confluence, adherent cells were dissociated with trypsin-EDTA and subcultured at a 1:3 ratio to maintain logarithmic growth.

Treatment of KGN cells. KGN cells were stimulated with dihydrotestosterone (DHT; cat. no. 15874; Cayman Chemical Company) at various concentrations (0, 10, 50, 100, 500, 1,000 and 2,000 nM) at 37˚C for 24 h, and the optimum concentration was selected for subsequent experiments. In addition, KGN cells were exposed to MT (cat. no. M5250; Sigma-Aldrich; Merck KGaA) at concentrations of 0, 0.1 and 10 pM, 1 and 100 nM at 37˚C for 48 h, and the optimum concentration (10 pM) was selected for subsequent experiments. In addition, KGN cells were first exposed to 100 nM DHT for 24 h followed by treatment with or without MT (10 pM) for an additional 48 h at 37˚C. To investigate the effect of MT on SIRT3 expression in human ovarian CGCs, CGCs obtained from control subjects and patients with PCOS were cultured *in vitro*. The cells were treated with 10 pM MT at 37˚C for 48 h, after which, the cells were harvested, and SIRT3 protein expression levels were measured using western blot analysis.

Cell transfection. Cells were transfected with SIRT3 overexpression plasmids (pCMV6-Entry backbone, Myc-DDK-tagged) purchased from OriGene Technologies, Inc. (cat. no. RC200190), or with an empty pCMV6-Entry plasmid in the negative control (NC) group, using Lipofectamine® 3000 (cat. no. L3000015; Invitrogen; Thermo Fisher Scientific, Inc.) according to the manufacturer's instructions. Briefly, when the KGN cell density reached 70-80%, transient transfection was performed; 4 μg plasmid solution was diluted with serum-free medium and gently mixed, and P3000 (supplied with Lipofectamine 3000) was added. Lipofectamine 3000 was equilibrated to room temperature and gently mixed with serum-free Opti-MEM® (cat. no. 31985; Gibco; Thermo Fisher Scientific, Inc.), followed by incubation at room temperature for 5 min to allow complex formation. Subsequently, the plasmid DNA solution was diluted in an equal volume of Opti-MEM and combined with the lipid mixture (Lipofectamine 3000 and Opti-MEM). The DNA-lipid complexes were allowed to form through a 10-min incubation at room temperature, after which, they were added dropwise to the cell culture dish using a sterile pipette. The dish was gently agitated to ensure an even distribution of the transfection mixture and was then transferred to a humidified 37˚C incubator containing 5% CO_2 for 4 h. Following this incubation period, the transfection medium was replaced with complete growth medium supplemented with 10% FBS, and the cells were maintained under standard culture conditions for an additional 24 h prior to an efficiency assessment through western blot analysis. For the inhibitor experiments, the cells were treated with the SIRT3 inhibitor 3-TYP (50 μM cat. no. 29660; Cayman Chemical Company) for 4 h at 37˚C.

Chemical treatment. KGN cells were treated with 100 nM DHT at 37˚C for 24 h to establish the DHT-induced model, followed by transfection with the SIRT3 overexpression plasmid for at 37˚C for 4 h. After transfection, the medium was replaced, and the cells were cultured for an additional 48 h. Then, chloroquine (CQ; 50 μM; cat. no. C6628; Sigma-Aldrich; Merck KGaA) was added for 4 h at 37˚C before cell collection. The protein expression levels of LC3 and P62 were subsequently detected by western blotting.

Cell counting Kit (CCK)-8 assay. A CCK-8 assay (cat. no. CA1211; Beijing Solarbio Science & Technology Co., Ltd.) was used to measure the viability of CGCs, according to the manufacturer's instructions. Briefly, the cells were seeded on 96-well plates at a density of $2x10^4$ cells/well, after which, 10 μl CCK8 reagent was added to the culture medium and the plate was incubated for 1.5 h. Finally, the absorbance was detected at 450 nm using a microplate reader (SpectraMax® iD3; Molecular Devices, LLC). The inhibition rate was calculated as follows: Inhibition rate (%)=[(OD control-OD treatment)/(OD control-OD blank)] x100. All CCK-8 assays were performed in triplicate and repeated three times.

ELISA. The collected FF was centrifuged at 400 x g for 10 min at room temperature, after which the cell-free supernatant was collected as the FF sample and stored at -80˚C for subsequent assays. The MT content of FF was measured using a Human MT ELISA Kit (cat. no. EH3344; Wuhan Fine Biotech Co., Ltd.), according to the manufacturer's instructions.

Measurement of reactive oxygen species (ROS) levels. KGN cells ($1x10^4$ cells/well) were loaded with 10 μmol/l dichlorodihydrofluorescein diacetate (DCFH-DA; Beyotime Biotechnology) by incubation at 37˚C for 20 min. Subsequently, the fluorescence intensity was quantified using a SpectraMax iD3 multifunctional microplate reader with excitation/emission wavelengths set at 488/525 nm.

MMP detection. The MMP of KGN cells was measured using the JC-1 fluorescent probe (Cayman Chemical Company). KGN cells ($1x10^5$ cells/well) were seeded in 24-well plates. After 24 h of culture, the cells were subjected to cell transfection or exposure to 10 pM MT as aforementioned, and then labelled with 10 μmol/l JC-1 for 20 min in an atmosphere containing 5% CO_2 at 37˚C. Fluorescence images were captured using an Image Xpress confocal microscope (Molecular Devices, LLC) to visualize both green (monomeric) and red (aggregated) fluorescence. For each group, 5-6 fields were randomly selected at low magnification by researchers who were blinded to the experimental groups to avoid selection bias. The total red and green fluorescence intensities in each field were measured using ImageJ software (version 1.51; National Institutes of Health), and MMP is expressed as a red/green fluorescence ratio. The data were obtained from at least three independent experiments.

Mito-Tracker Red CMXRos staining. Active mitochondria were labelled using Mito-Tracker Red CMXRos (Invitrogen; Thermo Fisher Scientific, Inc.). KGN cells ($1x10^5$ cells/well) were seeded in 24-well plates. After 24 h of culture, the cells were subjected to cell transfection or exposure to 10 pM MT as aforementioned, and were then incubated with 10 μM MitoTracker Red CMXRos staining solution at 37˚C for 20 min. After incubation, the cells were washed three times with PBS (Wuhan Servicebio Technology Co., Ltd.) and maintained in fresh culture medium. The fluorescence intensity was detected with an Xpress confocal microscope. For each group, 5-6 fields were randomly selected at low magnification by researchers who were blinded to group allocation. The

mean red fluorescence intensity per field was measured using ImageJ software (version 1.51) to determine the mitochondrial mass. The data were obtained from at least three independent experiments.

Western blotting. CGCs and KGN cells were homogenized in RIPA buffer (cat. no. RW0001; Hebei Ruipate Bio & Technology Co., Ltd.) and the protein concentration was determined using a BCA kit. Protein samples (5-8 μg) were then separated by SDS-PAGE on 10% gels and transferred to a polyvinylidene fluoride membrane (Sigma-Adrich; Merck KGaA). Subsequently, a blocking buffer containing 5% non-fat dried milk (Inner Mongolia Yili Industrial Group Company Ltd.) was used for 1.5 h at room temperature. The membrane was then incubated with primary antibodies against SIRT3 (1:1,000; cat. no. ab217319; Abcam), optic atrophy 1 (OPA1; 1:500; cat. no. ET1705-9; Huabio), DRP1 (1:1,000; cat. no. IPB0168; Baijia), phosphorylated (P)-DRP1 (Ser^{616}) (1:1,000; cat. no. AF8470; Affinity Biosciences), mitofusin 2 (MFN2; 1:1,000; cat. no. 9482S; Cell Signaling Technology, Inc.), FIS1 (1:500; cat. no. ET7109-17; Huabio), P62 (1:2,000; cat. no. PM045; MBL International Co.), LC3 (1:500; cat. no. PM036; MBL International Co.), and β-actin (1:5,000; cat. no. AC026; ABclonal Biotech Co., Ltd.) overnight at 4˚C. Following the primary antibody incubation, the membrane was incubated with HRP-goat anti-rabbit IgG (1:3,000; cat. no. RS0002; ImmunoWay Biotechnology Company) or HRP-goat anti-mouse IgG (1:3,000; cat. no. S1001; Hebei Ruipate Bio & Technology Co., Ltd.). The protein bands were visualized using an ECL detection reagent (Shanghai Yeasen Biotechnology Co., Ltd.) on the Minichemi 320 chemiluminescence imaging system (Beijing Sage Creation Science Co., Ltd.) and protein levels were semi-quantified with ImageJ (version 1.51) software.

Statistical analysis. Data are presented as the mean ± SD for normally distributed data, or as median (interquartile range) for non-normally distributed data. Statistical analyses were performed using SPSS 26.0 software (IBM Corp.). Normality of the data distribution was assessed using the Shapiro-Wilk test. For data following a normal distribution with homogeneous variances, parametric tests were applied; comparisons between two groups were performed using an independent sample t-test, whereas comparisons among multiple groups were performed using one-way ANOVA followed by Tukey's post hoc test. For data that did not follow a normal distribution or with unequal variances, nonparametric tests were applied; comparisons between two groups were performed using Mann-Whitney U test, whereas comparisons among multiple groups were performed using Kruskal-Wallis test followed by the Dunn-Bonferroni test for post hoc pairwise comparisons. Each experiment was repeated using at least three independent primary CGC samples (biological replicates, n ≥3 per group), and each biological replicate was measured in two technical replicates. Due to inherent limitations in obtaining primary CGCS, sample sizes varied across different detection markers; detailed sample sizes are provided in the Results section and corresponding figure legends. $P<0.05$ was considered to indicate a statistically significant difference.

Results

Comparison of clinical characteristics and hormone levels between the PCOS and control groups. The clinical characteristics of the study population are summarized in Table I. A total of 36 women with PCOS and 42 age-matched controls were included in the analysis. No significant differences were observed between the two groups regarding age, body mass index, baseline oestradiol and progesterone levels, metaphase II oocyte rate, fertilization rate or high-quality embryo rate. However, distinct endocrine profiles were observed: Compared with in the control group, the PCOS group had significantly elevated baseline testosterone levels, increased luteinizing hormone (LH) concentrations and a significantly higher LH/follicle-stimulating hormone (FSH) ratio. Conversely, basal serum FSH and prolactin levels were notably lower in patients with PCOS.

CGCs from patients with PCOS exhibit mitochondrial dysfunction and aberrant autophagy activation. To investigate mitochondrial dynamics in CGCs, western blot analysis was performed on samples obtained from 9 patients with PCOS and 9 control patients. Owing to the limited protein yield from CGCs, the effective sample size for certain markers was smaller than that of the initial cohort ($n<9$), and specific sample sizes are indicated in the corresponding results. The protein levels of DRP1, MFN2, OPA1, FIS1 and P-DRP1 (Ser^{616}) were detected by western blotting. The results revealed that the expression levels of MFN2 and OPA1 were significantly lower in the PCOS group than in the control group (Fig. 1A). Conversely, the expression level of FIS1 and the ratio of P-DRP1 (Ser^{616})/total DRP1 were significantly increased in the PCOS group. These findings indicated a pronounced imbalance in mitochondrial dynamics in CGCs derived from patients with PCOS, characterized by increased fission and decreased fusion. In addition, SIRT3 protein levels were significantly lower in the CGCs from the PCOS group compared with those from the control group, as determined by western blotting, suggesting that SIRT3 downregulation may contribute to mitochondrial dysfunction in PCOS GCs (Fig. 1C).

To evaluate autophagic activity in the CGCs of patients with PCOS, autophagic vesicles were observed under electron microscopy (Fig. 1B). The results revealed an increased number of autophagic vesicles within the ovarian CGCs of patients with PCOS, suggesting that autophagy may be increased in the CGCs of patients with PCOS.

Furthermore, the expression levels of autophagy-related markers, LC3 and P62, were analysed. Compared with those in the control group, the PCOS group exhibited a significantly increased LC3II/I ratio and significantly decreased P62 expression levels (Fig. 1C), indicating that autophagic activity was enhanced in the CGCs of patients with PCOS.

SIRT3 overexpression enhances mitochondrial function and suppresses autophagy in DHT-treated KGN cells. The granulosa-like tumour cell line KGN, which retains its steroidogenic capacity and serves as a robust model for human GC research (22), was used to establish an *in vitro* PCOS model through DHT induction, a widely adopted approach

Table I. Comparison of the general condition between the two patient groups.

Characteristic	CON group (n=41)	PCOS group (n=36)	P-value
Age, years	31.17±3.30	31.47±3.31	0.691
BMI, kg/m^2	24.40±3.95	26.24±4.85	0.07
Basal FSH, IU/l	7.07±1.67	6.22±1.81	0.034[a]
Basal LH, IU/l	4.28±1.84	6.08±3.25	0.003[a]
LH/FSH	0.63±0.29	1.00±0.55	0.001[a]
Basal E2, pg/ml	38.96±12.36	36.80±12.73	0.453
Basal P, ng/ml	0.62±0.37	0.64±0.88	0.871
PRL, ng/ml	15.21±7.83	11.27±4.89	0.011[a]
Basal T, ng/ml	0.38±0.19	0.48±0.24	0.049[a]
MII rate	0.84±0.10	0.77±0.22	0.076
Fertilization rate	0.87±0.15	0.87±0.20	0.845
Excellent embryo rate	0.60±0.27	0.57±0.24	0.591

Data are presented as the mean ± SD. [a]P<0.05. MII rate=(number of MII)/(total number of oocytes retrieved); fertilization rate=(fertilized oocytes)/(MII oocytes inseminated); excellent embryo rate=(grade I/II embryos)/(fertilized embryos). BMI, body mass index; FSH, follicle-stimulating hormone; LH, luteinizing hormone; MII, metaphase II; E2, oestradiol; P, progesterone; PRL, prolactin; T, testosterone.

in PCOS studies (23-25). To optimize the treatment conditions, KGN cells were exposed to increasing concentrations of DHT (0-2,000 nM) for 24 h. CCK-8 analyses revealed that DHT inhibited cell viability in a concentration-dependent manner (Fig. 2A). Notably, treatment with 100 nM DHT reduced cell viability by ~50%. Western blot analysis was then performed to assess the protein expression levels of SIRT3, mitochondrial fission/fusion markers (OPA1, DRP1 and MFN2) and P62 in KGN cells treated with various concentrations of DHT (Fig. 2B). Consistent with the expression patterns observed in GCs from patients with PCOS, 100 nM DHT markedly downregulated SIRT3, DRP1, OPA1, MFN2 and P62 expression compared with in the untreated control group. Therefore, this concentration was selected for subsequent experiments.

To investigate the functional role of SIRT3 in DHT-treated KGN cells, SIRT3 overexpression was used to assess mitochondrial function. Firstly, successful SIRT3 overexpression in KGN cells was confirmed, with protein levels increasing ~2-fold relative to those in the NC cells (Fig. 2C), thereby validating the transfection efficiency.

SIRT3 modulates MMP and dynamics (26); therefore, to evaluate the regulatory role of SIRT3 in mitochondrial function, three experimental groups were analysed: Untreated control, DHT-treated and DHT + SIRT3 groups. The MMP was assessed using JC-1 staining. Cells with a low MMP contained JC-1 monomers and exhibited green fluorescence signals, whereas those with a high MMP showed red fluorescence signals due to JC-1 polymer formation. JC-1 staining revealed a significant reduction in the MMP in DHT-treated cells compared with that in the control group, whereas this effect was partially reversed by SIRT3 overexpression (Fig. 2D). By contrast, MitoTracker staining revealed no significant differences in mitochondrial fluorescence intensity across groups, suggesting that mitochondrial mass remained unchanged (Fig. 2E).

DHT treatment significantly reduced the protein levels of the mitochondrial fusion proteins OPA1 and MFN2 and increased the P-DRP1 (Ser^{616})/DRP1 ratio (Fig. 2F). Notably, SIRT3 overexpression in DHT-treated cells upregulated OPA1 and MFN2 expression (P<0.05 vs. DHT) and decreased the P-DRP1 (Ser^{616})/DRP1 ratio, suggesting that SIRT3 may enhance mitochondrial function. The expression levels of autophagy-associated proteins were assessed by western blotting. DHT treatment significantly reduced the protein levels of the autophagic substrate P62 (Fig. 2G), indicating increased autophagic flux. Notably, SIRT3 overexpression in DHT-treated cells significantly increased P62 expression compared with DHT alone, suggesting impaired autophagic flux. LC3-II levels showed an increasing trend in both DHT and DHT + SIRT3 groups, but the changes were not statistically significant. As shown in Fig. 2G, overexpression of SIRT3 in DHT-treated cells led to elevated P62 levels, which appears to exert an opposite effect to DHT. It remains unclear whether SIRT3 overexpression inhibits autophagic flux, selectively regulates mitophagy without affecting general autophagy, or induces compensatory changes in P62 synthesis. To definitively address this issue, autophagic flux was analysed in KGN cells using CQ. CQ blocks lysosomal degradation, so the extent of LC3-II and P62 accumulation in the presence of CQ is proportional to autophagic flux; a greater accumulation reflects higher autophagic flux. The cells were divided into the following six groups: Control, control + CQ, DHT, DHT + CQ, DHT + SIRT3 and DHT + SIRT3 + CQ, and the accumulation of LC3II and P62 in the presence of CQ was compared. The accumulation of LC3II and P62 in the DHT + CQ group was significantly greater than that in the control + CQ group, confirming that DHT increased autophagic flux (Fig. 2H). Furthermore, the accumulation of LC3II and P62 in the DHT + SIRT3 + CQ group was significantly lower than that in the DHT + CQ group, indicating that SIRT3 overexpression inhibited the DHT-mediated increase in autophagic flux.

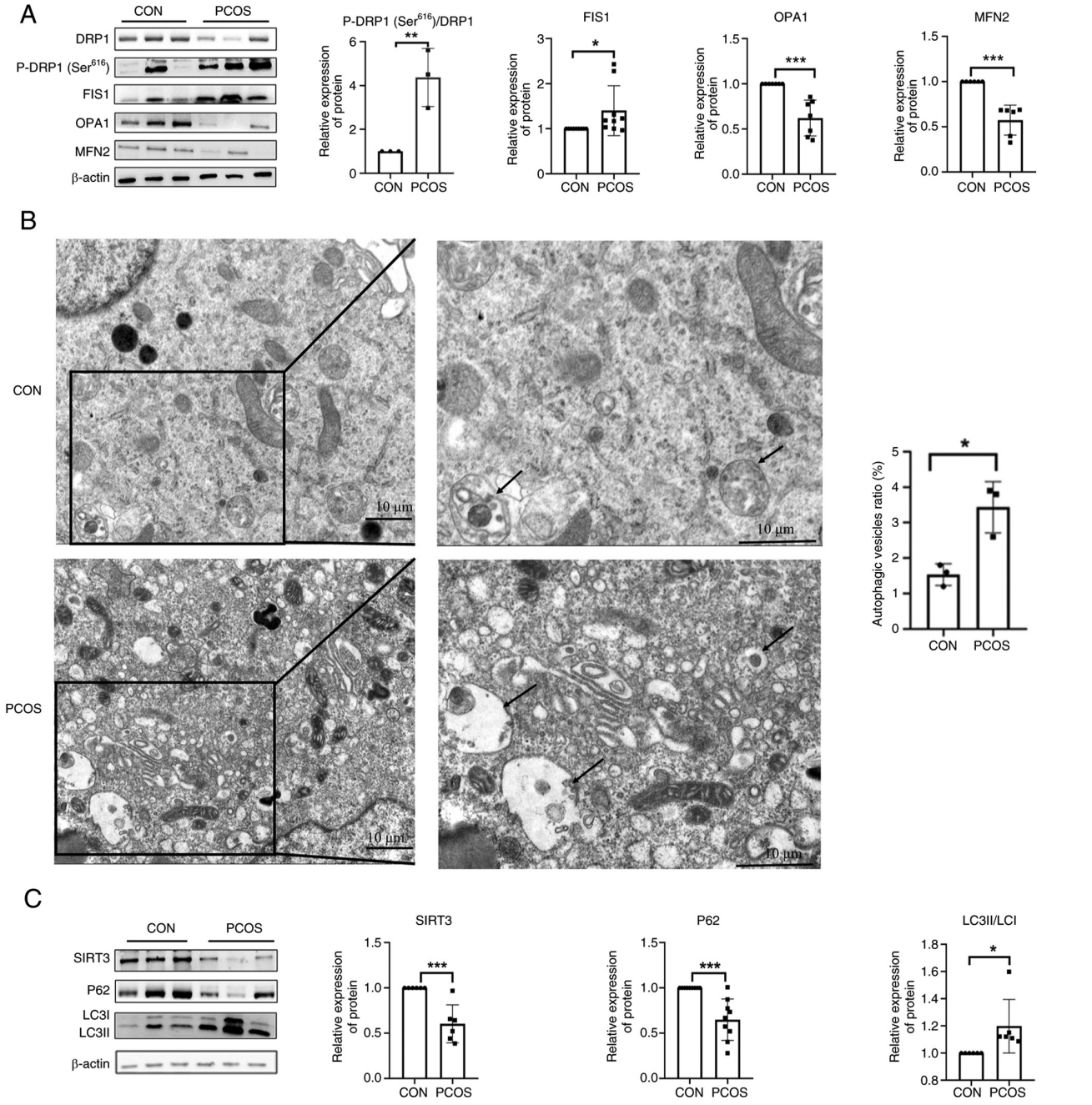

Figure 1. CGCs from patients with PCOS exhibit mitochondrial dysfunction and aberrant autophagy activation. (A) Abnormal expression of mitochondrial fusion/fission proteins in the CGCs of patients with PCOS. Protein levels of MFN2 (n=6 patients), OPA1 (n=7 patients), FIS1 (n=9 patients), DRP1 (n=6 patients) and P-DRP1 (Ser^{616}) (n=3 patients) were detected by western blotting in CGCs from patients with PCOS and controls. (B) Ultrastructural evidence of autophagic activation and the autophagic vesicle ratio in CGCs from patients with PCOS and controls. Transmission electron micrographs showing increased autophagosome density (black arrows) in PCOS CGCs (n=3) compared with controls (n=3). Scale bar, 10 μm. (C) Western blot analysis of autophagy-related markers in CGCs from patients with PCOS and controls. Western blot analysis revealed reduced SIRT3 (n=6) and P62 (n=9) expression, with a concomitant increase in the LC3-II/I ratio (n=6) in PCOS CGCs compared with the controls. *P<0.05, **P<0.01, ***P<0.001. CON, control; CGC, cumulus granulosa cell; DRP1, dynamin-related protein 1; FIS1, mitochondrial fission 1 protein; MFN2, mitofusin 2; OPA1, optic atrophy 1; P-, phosphorylated; PCOS, polycystic ovary syndrome; SIRT3, sirtuin 3.

MT upregulates SIRT3 in CGCs and protects mitochondrial function in DHT-induced KGN cells. To assess MT levels in patients with PCOS, the concentrations of MT in the FF were measured using ELISA. Compared with in the FF from control patients, the FF from patients with PCOS had significantly lower MT levels (172.7±51.63 vs. 205.02±59.87 pg/ml; Fig. 3A).

To investigate the regulatory effect of MT on SIRT3 expression, KGN cells were cotreated with 100 nM DHT and various concentrations of MT; the results revealed that treatment with 10 pM MT significantly increased SIRT3 expression compared with DHT (Fig. 3B).

In human CGCs, SIRT3 protein levels were significantly lower in PCOS-derived CGCs than in control CGCs. By contrast, MT treatment of CGCs form patients with PCOS (PCOS + MT group) restored SIRT3 expression to near-control levels (Fig. 3C).

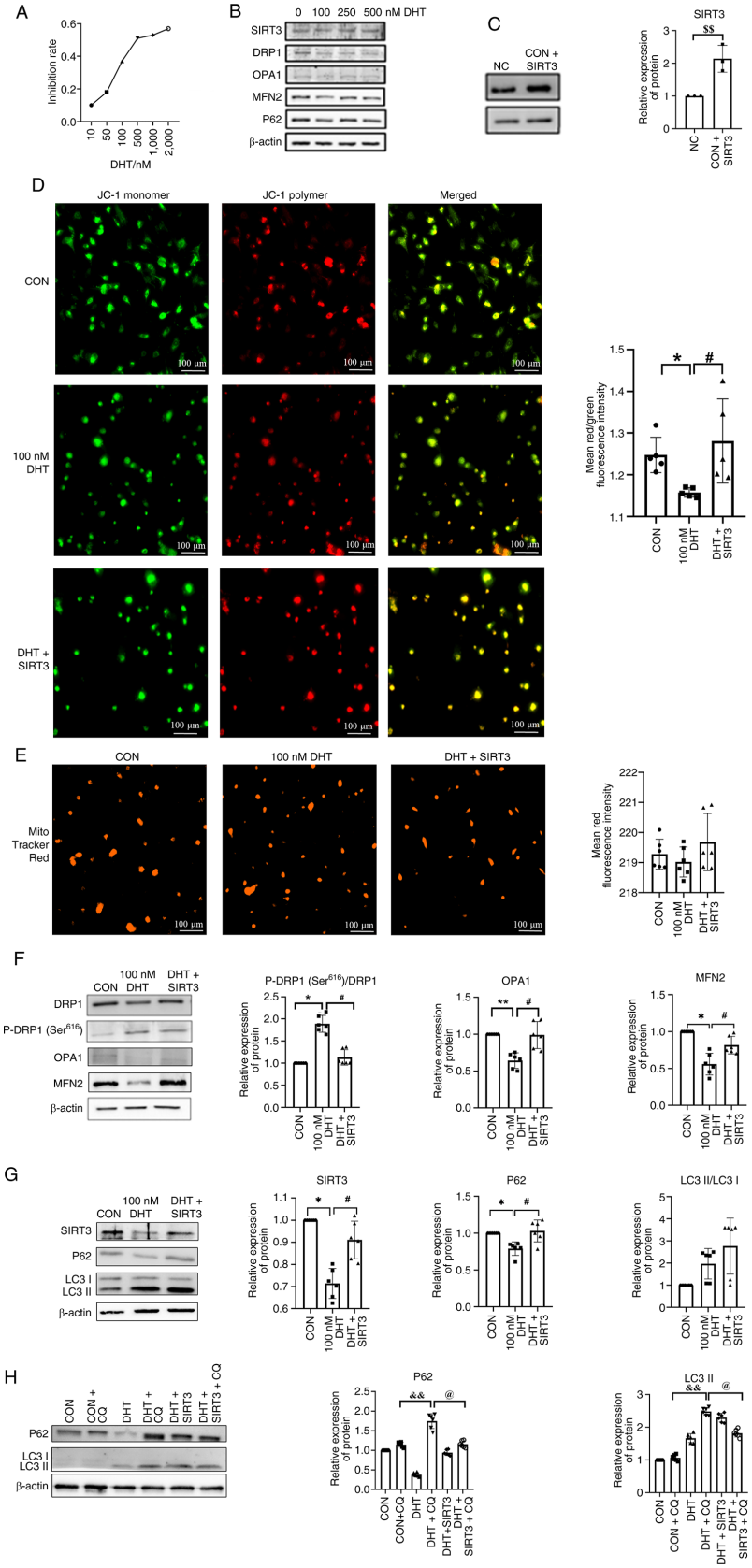

Figure 2. SIRT3 overexpression enhances mitochondrial function and suppresses autophagy in KGN cells. (A) Effect of different concentrations of DHT on KGN cell viability (n=6). (B) Expression of mitochondrial dynamics-related proteins SIRT3, DRP1, P-DRP1 (Ser^{616}), MFN2 and OPA1 in response to 0, 100, 250 and 500 nM DHT, as detected by western blotting (n=6). (C) Western blot analysis to assess the expression levels of SIRT3 in SIRT3-overexpressing KGN cells, confirming transfection efficiency. (D) Mitochondrial membrane potential in KGN cells overexpressing SIRT3 (n=5) Scale bars, 100 μm. (E) Effect of SIRT3 overexpression on the number of mitochondria (n=6). Scale bars, 100 μm. Expression levels of (F) mitochondrial dynamics-related proteins [SIRT3, DRP1, P-DRP1 (Ser^{616}), MFN2 and OPA1], and (G) LC3 and P62 were detected by western blotting (n=6). (H) Expression levels of LC3-II and P62 in the presence of CQ was detected by western blotting (n=6). *P<0.05, **P<0.01 vs. CON group; $^{\#}$P<0.05 vs. DHT group, $^{\$\$}$P<0.01 vs. NC group; $^{\&\&}$P<0.01 vs. CON + CQ group, $^{@}$P<0.05 vs. DHT + CQ group. CON, control; CQ, chloroquine; DHT, dihydrotestosterone; DRP1, dynaminrelated protein 1; FIS1, mitochondrial fission 1 protein; MFN2, mitofusin 2; NC, negative control; OPA1, optic atrophy 1; P-, phosphorylated; SIRT3, sirtuin 3.

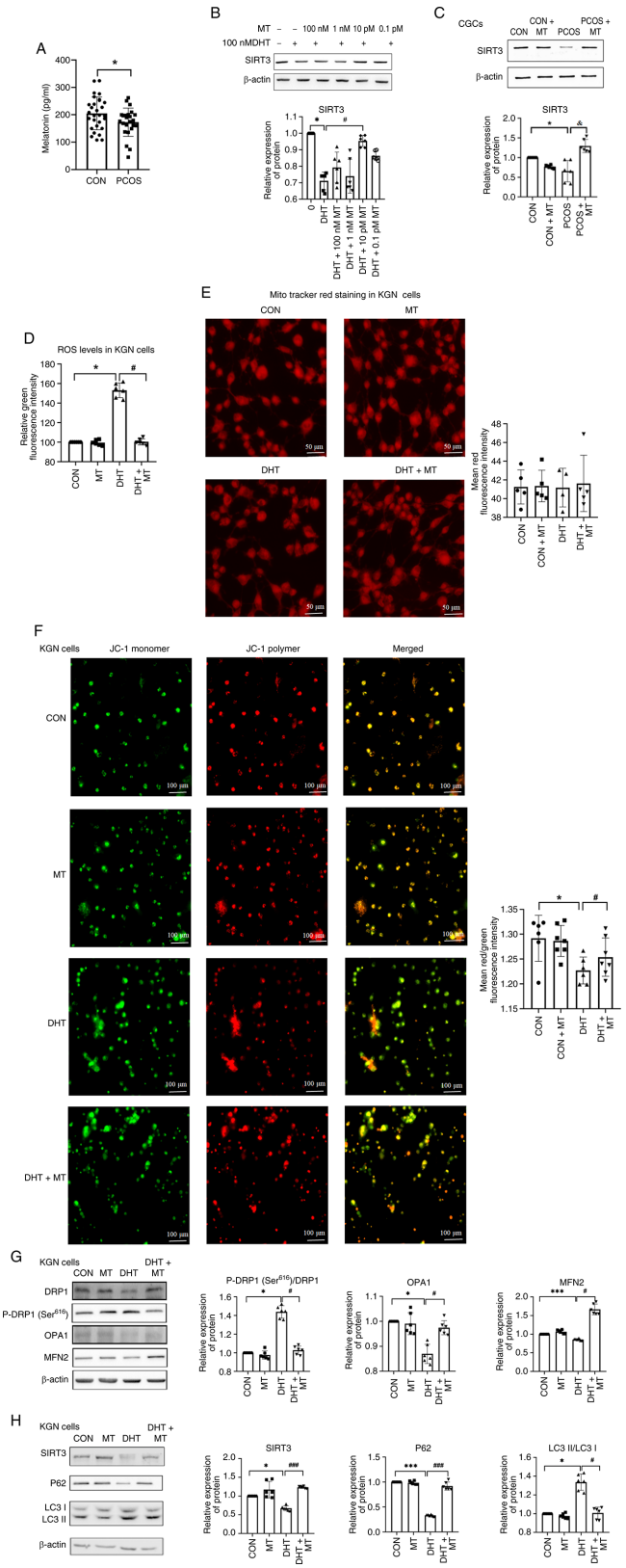

Figure 3. MT upregulates SIRT3 in CGCs and protects mitochondrial function in DHT-induced KGN cells. (A) Comparison of MT levels in the follicular fluid between the two groups of patients (n=29 vs. n=24). (B) KGN cells were cultured with different concentrations of MT, and the expression of SIRT3 was compared (n=6). (C) Protein expression levels of SIRT3 in CGCs of the four groups (n=6). (D) ROS levels in KGN cells from the four groups. Dichlorodihydrofluorescein diacetate staining was performed to measure the concentrations of ROS in those groups, and the staining was detected using a microplate reader (n=6). (E) Changes in fluorescence intensity were observed using MitoTracker Red dye (n=5). Scale bar, 50 μm. (F) MMP detected with Image Xpress confocal microscopy and analysis of MMP by JC-1 staining in CGCs from the CON group, CON + MT group, DHT group and DHT + MT group (n=6). Scale bar, 100 μm. Western blot analysis of (G) DRP1, P-DRP1Ser^{616}, OPA1 and MFN2, and (H) SIRT3, P62 and LC3 expression in the CON group, CON + MT group, DHT group and DHT + MT group (n=6). *P<0.05, ***P<0.001 vs. CON group; $^{\#}$P<0.05, $^{\#\#\#}$P<0.001 vs. DHT group, $^{\&}$P<0.05 vs. PCOS + MT. CON, control; CGC, cumulus granulosa cell; DHT, dihydrotestosterone; DRP1, dynaminrelated protein 1; FIS1, mitochondrial fission 1 protein; MFN2, mitofusin 2; MMP, mitochondrial membrane potential; MT, melatonin; OPA1, optic atrophy 1; P-, phosphorylated; PCOS, polycystic ovary syndrome; ROS, reactive oxygen species; SIRT3, sirtuin 3.

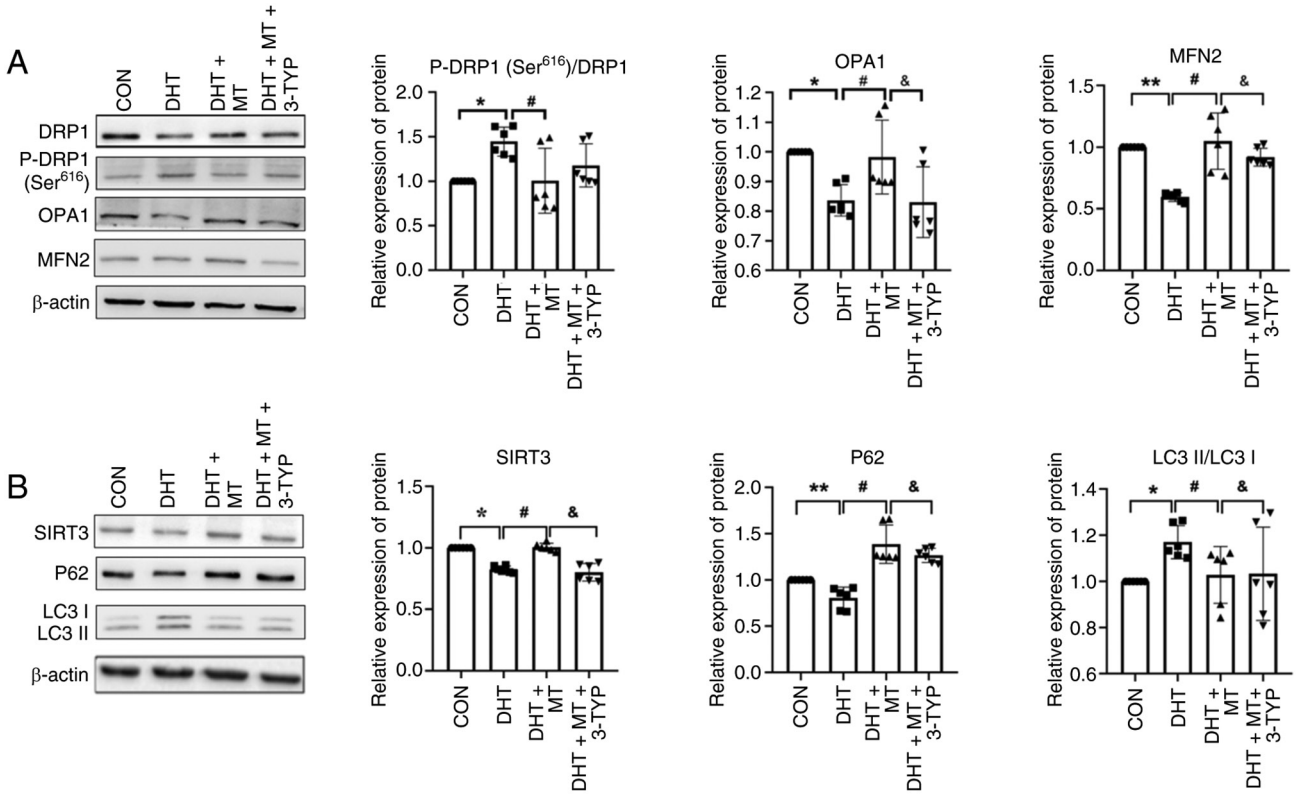

Figure 4. A SIRT3 inhibitor abrogates the effects of MT on mitochondrial dynamics and autophagy. Western blot analysis of (A) DRP1, P-DRP1 (Ser^{616}), OPA1 and MFN2 expression, and (B) SIRT3, P62 and LC3 expression (n=6). Data are presented as the mean ± SD. *P<0.05, **P<0. vs. CON group; $^{\#}$P<0.05 vs. DHT group; $^{\&}$P<0.05 vs. DHT+MT group. CON, control; DHT, dihydrotestosterone; DRP1, dynamin-related protein 1; MFN2, mitofusin 2; MT, melatonin; OPA1, optic atrophy 1; P-, phosphorylated; SIRT3, sirtuin 3.

To assess the effect of MT on mitochondrial homeostasis, the intracellular ROS levels in DHT-induced KGN cells were measured by DCFH-DA staining. Notably, ROS levels were increased in the DHT group, whereas this increase was normalized by cotreatment with MT (Fig. 3D). Mito Tracker Red staining revealed no significant differences in mitochondrial mass among the groups (control, control + MT, DHT and DHT + MT; Fig. 3E). However, JC-1 staining revealed a decrease in the MMP in DHT-treated cells, which was effectively restored by MT (Fig. 3F).

Western blot analysis of mitochondrial dynamics-related proteins revealed that DHT increased P-DRP1 (Ser^{616}) levels, and reduced MFN2 and OPA1 levels, all of which were normalized by MT cotreatment (Fig. 3G). These results suggested that MT may ameliorate the DHT-induced abnormalities in mitochondrial dynamics.

DHT exposure decreased P62 and SIRT3 levels, and increased the LC3-II/I ratio, whereas MT treatment reversed these effects (Fig. 3H). Together, these findings suggested that MT alleviates DHT-induced mitochondrial dysfunction by modulating SIRT3 expression and regulating mitophagy.

SIRT3 inhibition abrogates the effects of MT on mitochondrial dynamics and autophagy. To further verify whether MT regulates mitochondrial dynamics by upregulating SIRT3 expression, KGN cells were treated with or without DHT for 24 h, then treated with the SIRT3-specific inhibitor 3-TYP for 4 h, followed by treatment with MT for 48 h. KGN cells were divided into four groups: Control, DHT, DHT + MT and DHT + MT + 3-TYP, and the expression levels of mitochondrial dynamics-associated proteins were assessed by western blotting. The results showed that the protein expression levels of OPA1 and MFN2 in the DHT + MT group were significantly higher than those in the DHT group, but were significantly reduced after the addition of the SIRT3 inhibitor 3-TPY (Fig. 4A). The ratio of P-DRP1 (Ser^{616})/DRP1 in the DHT + MT group was significantly lower than that in the DHT group; however, the addition of the SIRT3 inhibitor did not alter this ratio. This revealed that MT failed to reverse the DHT-induced abnormalities in mitochondrial fusion when SIRT3 expression was inhibited, suggesting that SIRT3 is essential for MT-mediated regulation of mitochondrial fusion.

To verify whether MT alleviates DHT-induced autophagic dysfunction through upregulation of SIRT3 expression, the expression of autophagy-related markers was assessed by western blotting. Following SIRT3 inhibition, MT was unable to suppress excessive autophagy (Fig. 4B). These findings further support that MT may restore mitochondrial dynamics and autophagic activity by increasing SIRT3 expression.

Discussion

The primary clinical manifestation in patients with PCOS is anovulation, which primarily results from impaired follicular development and arrested maturation. As critical regulators of primordial follicle activation during folliculogenes (27), ovarian GCs substantially influence follicular initiation and maturation through the functional integrity of their mitochondria. Previous investigations have demonstrated marked

mitochondrial dysfunction in CGCs derived from patients with PCOS, characterized by a decreased MMP, excessive accumulation of ROS and dysregulation of mitochondrial biogenesis pathways (28,29). Given the essential role of CGC mitochondria in coordinating follicular development and oocyte competence, the precise pathophysiological mechanisms linking PCOS-associated mitochondrial abnormalities to impaired oocyte quality remain incompletely understood. This highlights the critical need to elucidate the molecular cascades through which PCOS compromises oocyte developmental potential while also exploring innovative strategies to optimize reproductive outcomes in this prevalent endocrine disorder.

Mitochondrial dynamics and damage exhibit a tightly coupled bidirectional relationship (30). Mitochondrial impairment can disrupt dynamic equilibrium, thereby compromising cellular energy homeostasis, apoptotic regulation and other critical biological processes, whereas aberrant mitochondrial dynamics may conversely exacerbate mitochondrial damage (31). Upon phosphorylation at Ser616, DRP1 is activated and translocates to the mitochondria, where it binds protein partners located on the outer mitochondrial membrane and subsequently promotes mitochondrial fission (32). The findings of the present study revealed significant downregulation of the mitochondrial fusion regulators MFN2 and OPA1, indicating a reduction in mitochondrial fusion in the CGCs of patients with PCOS. Activation of P-DRP1 (Ser616) facilitates the translocation of DRP1 to the mitochondria, and an increased P-DRP1 (Ser^{616})/DRP1 ratio promotes mitochondrial fission, leading to enhanced mitochondrial division, thereby contributing to an imbalance in mitochondrial dynamics in the context of PCOS. Notably, SIRT3 expression was markedly reduced in the CGCs of patients with PCOS. Experimental evidence has demonstrated that SIRT3 deficiency exacerbates mitochondrial dysfunction, whereas its upregulation restores mitochondrial dynamics in renal tubular systems (33). The pathological triad of oxidative stress, mitochondrial injury and SIRT3 depletion has been mechanistically linked, with SIRT3 supplementation showing therapeutic potential in ameliorating renal damage in murine models of acute kidney injury (34). These findings collectively suggest that SIRT3 downregulation may constitute a central mechanistic node underlying mitochondrial dynamic disturbances in PCOS CGCs; thus, a novel therapeutic axis for addressing ovarian dysfunction in this syndrome is proposed.

Accumulating evidence highlights the critical role of SIRT family proteins, particularly the understudied protein SIRT3, in the pathogenesis of PCOS. While SIRT1 remains the focus of current research, the current clinical data revealed significant SIRT3 downregulation in patients with PCOS, which is consistent with the findings in a previous study that SIRT3 knockdown in KGN GCs mimics PCOS-associated glucose dysregulation and insulin resistance (29). Utilizing a DHT-induced *in vitro* model of PCOS, mitochondrial dysfunction was observed, as characterized by reduced MMP and elevated ROS levels, despite the unchanged mitochondrial mass. DHT concurrently disrupted mitochondrial dynamics by increasing fission and decreasing fusion while promoting mitophagy, as evidenced by reduced P62 levels. These results reveal a dual mechanism whereby hyperandrogenism induces mitochondrial pathology via SIRT3 deficiency-mediated fission and fusion imbalance and autophagic flux arrest, positioning SIRT3 as a therapeutic target for PCOS-related ovarian metabolic dysfunction.

The present study demonstrated that SIRT3 overexpression rescued mitochondrial homeostasis in KGN cells by counteracting DHT-induced dysfunction. In KGN cells, SIRT3 overexpression significantly increased the MMP, while normalizing mitochondrial dynamics by decreasing P-DRP1 (Ser^{616}) levels and increasing the expression of fusion regulators (MFN2 and OPA1). Previous studies have shown that SIRT3 can influence mitochondrial homeostasis by regulating upstream signalling molecules (such as AMPK/PGC-1α) or antioxidant enzymes (such as SOD2), thereby indirectly affecting the expression and function of dynamic proteins (35,36). Therefore, the changes in total protein levels observed in the current study may have resulted from the overall regulatory network of SIRT3. These findings suggest that SIRT3 mitigates PCOS-associated mitochondrial damage by restoring fission and fusion equilibrium. SIRT3 overexpression induced an increase in P62 levels, which indicates that it exerted an opposite effect to DHT treatment alone, because DHT alone decreased P62. To investigate whether the changes in P62 levels reflect alterations in autophagic flux, cells were treated with CQ and autophagic analysis was performed. The results of CQ treatment indicated that SIRT3 overexpression significantly reduced LC3-II and P62 accumulation in the DHT + SIRT3 + CQ group compared with in the DHT + CQ group. Thus, changes in P62 levels did reflect alterations in autophagic flux, and the findings indicated that SIRT3 suppressed the DHT-enhanced autophagic flux. SIRT3 may impair autophagic degradation efficiency, counteract DHT-induced autophagic overactivation and reduce autophagic flux.

MT, a lipophilic hormone synthesized by the pineal gland, exerts pleiotropic effects on cellular redox balance and mitochondrial homeostasis through its membrane permeability (37). Emerging evidence has suggested that MT deficiency is involved in ovarian dysfunction, with the present study confirming significantly reduced levels of MT in the FF of patients with PCOS compared with those in the control individuals. Mechanistically, exogenous MT treatment increased SIRT3 expression in the CGCs of patients with PCOS. By upregulating SIRT3 expression, MT reversed DHT-induced mitochondrial damage in CGCs, as evidenced by the restored membrane potential, attenuated oxidative stress, and normalized fission and fusion dynamics. Crucially, MT suppressed excessive autophagy, whereas the addition of a SIRT3 inhibitor abolished the beneficial effects of MT on mitochondrial dynamics and mitophagy, unequivocally indicating that SIRT3 is a key mediator of the therapeutic effect of MT. These findings align with clinical observations that MT supplementation alleviates PCOS-associated metabolic disturbances (38), positioning the MT-SIRT3 axis as a druggable pathway to counteract androgen-driven mitochondrial pathology in patients with PCOS. The present study revealed that MT significantly upregulated SIRT3 expression in CGCs; however, the upstream regulatory mechanism remains to be elucidated. The biological effects of MT are typically mediated through two pathways: One involves the activation of downstream signalling cascades (such as PI3K/Akt and

PKA/CREB) via the membrane receptors MT membrane receptor 1 and MT2, thereby regulating gene transcription (39,40); the other involves its role as a potent antioxidant, which reduces oxidative stress-induced damage to the SIRT3 protein by scavenging free radicals, thus indirectly maintaining its expression levels (41). Previous studies have reported that MT can activate the SIRT3 signalling axis through MT2 to ameliorate cardiomyocyte hypoxia/reoxygenation injury (20), and can also exert antioxidative, antiapoptotic and anti-inflammatory renoprotective effects via SIRT3 activation (42,43). Future studies employing specific receptor antagonists (such as luzindole) or antioxidant interventions will help to elucidate the relative contributions of these two mechanisms in GCs from patients with PCOS.

The present study identified the MT-SIRT3 axis as a pivotal regulatory node in PCOS-associated mitochondrial dysfunction, offering novel mechanistic insights into hyperandrogenism-driven ovarian metabolic dysregulation. The findings revealed that the SIRT3-dependent restoration of mitochondrial dynamics and mitophagy is central to the therapeutic effects of MT. However, the present study has several limitations. First, while the use of cell lines is valuable for obtaining mechanistic insights, it does not fully recapitulate the complex *in vivo* environment. Owing to the limited protein yield from primary CGCs, the sample size was relatively small, which may affect the generalizability of the findings. The results should be validated in future studies with larger sample sizes of primary GCs. Second, the lack of validation in an *in vivo* animal model of PCOS represents another key limitation. Although the DHT-treated KGN cell line serves as a well-established *in vitro* model for mechanistic studies, it cannot replicate the complex systemic interactions that characterize the pathophysiology of PCOS. Therefore, well-established PCOS animal models (such as letrozole-induced or DHT-induced rodent models) should be employed in future studies to validate the therapeutic efficacy of MT, and assess its long-term effects on ovarian function, metabolic parameters and reproductive outcomes. Third, MT is a circadian hormone with a typical nocturnal secretion pattern and its levels in FF may exhibit diurnal fluctuations. The current *in vitro* experiments employed constant MT treatment, which does not mimic the pulsatile or cyclical nature of MT exposure *in vivo*. Future studies should investigate whether the timing of MT administration affects its protective effects on the functions of CGCs. Finally, the mechanistic interaction between MT and SIRT3 was investigated primarily using pharmacological inhibition and overexpression strategies, without direct molecular binding assays (such as binding affinity determinations). Receptor blockade and antioxidant interventions should be performed in future studies for in-depth analysis. Moreover, molecular docking assays should be prioritized to map MT-SIRT3 binding interfaces coupled with multiomics profiling to decode downstream deacetylation targets. These insights pioneer a paradigm shift towards precision interventions targeting mitochondrial epigenetics in PCOS while underscoring the importance of pharmacokinetic optimization to harness the full therapeutic potential of this pathway.

Acknowledgements

Not applicable.

Funding

The present study was supported by the Government Clinical Medical Talent Training Program (grant nos. ZF2026372 and ZF2026373).

Availability of data and materials

The data generated in the present study may be requested from the corresponding author.

Authors' contributions

CX, ZL, TC, HL, XZ, WY, JZ, DS and XW contributed to study conception and design. CX and TC performed the experiments. XZ, WY and JZ were responsible for the collection of CGCs. ZL and HL performed the data collection. DS and ZL analysed the data. CX and ZL wrote the first draft of the manuscript, and all authors commented on previous versions of the manuscript. DS and XW confirm the authenticity of all the raw data. All the authors read and approved the final manuscript.

Ethics approval and consent to participate

The present study was approved by the Ethics Committee of the Hebei Reproductive Health Hospital (approval no. KYY-2021-LW-008; Shijiazhuang, China). Written informed consent was obtained from each patient after a full explanation of the purpose and nature of all the procedures used. The procedures of the present study were in accordance with the ethical standards stated in The Declaration of Helsinki (1964).

Patient consent for publication

Not applicable.

Competing interests

The authors declare that they have no competing interests.

References

1. Zhang Y, Chen ZJ and Zhao H: Polycystic ovary syndrome: A metabolic disorder with therapeutic opportunities. Cell Metab 37: 1932-1949, 2025.
2. Gao Y, Zou Y, Wu G and Zheng L: Oxidative stress and mitochondrial dysfunction of granulosa cells in polycystic ovarian syndrome. Front Med (Lausanne) 10: 1193749, 2023.
3. Alberico HC and Woods DC: Role of granulosa cells in the aging ovarian landscape: A focus on mitochondrial and metabolic function. Front Physiol 12: 800739, 2021.
4. Schmalbrock LJ, Weiss G, Rijntjes E, Reinschissler N, Sun Q, Schenk M and Schomburg L: Pronounced trace element variation in follicular fluids of subfertile women undergoing assisted reproduction. Nutrients 13: 4134, 2021.
5. Sreerangaraja Urs DB, Wu WH, Komrskova K, Postlerova P, Lin YF, Tzeng CR and Kao SH: Mitochondrial function in modulating human granulosa cell steroidogenesis and female fertility. Int J Mol Sci 21: 3592, 2020.
6. Dabravolski SA, Nikiforov NG, Eid AH, Nedosugova LV, Starodubova AV, Popkova TV, Bezsonov EE and Orekhov AN: Mitochondrial dysfunction and chronic inflammation in polycystic ovary syndrome. Int J Mol Sci 22: 3923, 2021.

7. Delcour C, Amazitl, Patino LC, Magnin F, Fagart J, Delemer B, Young J, Laissue P, Binart N and Beau I: ATG7 and ATG9A loss-of-function variants trigger autophagy impairment and ovarian failure. Genet Med 21: 930-938, 2019.
8. Wang F, Han J, Wang X, Liu Y and Zhang Z: Roles of HIF-1α/BNIP3 mediated mitophagy in mitochondrial dysfunction of letrozole-induced PCOS rats. J Mol Histol 53: 833-842, 2022.
9. Liu H, Zang C, Yuan F, Ju C, Shang M, Ning J, Yang Y, Ma J, Li G, Bao X and Zhang D: The role of FUNDC1 in mitophagy, mitochondrial dynamics and human diseases. Biochem Pharmacol 197: 114891, 2022.
10. Poole LP and Macleod KF: Mitophagy in tumorigenesis and metastasis. Cell Mol Life Sci 78: 3817-3851, 2021.
11. Liu S, Huang Z, Yin Z, Chen L, Ye L, Zhang D and Bai X: Drp1 in Parkinson's disease: Mechanisms of disease pathology and the promise of targeted therapeutic strategies. Life Sci 384: 124086, 2026.
12. Cai C, Guo Z, Chang X, Li Z, Wu F, He J, Cao T, Wang K, Shi N, Zhou H, *et al*: Empagliflozin attenuates cardiac microvascular ischemia/reperfusion through activating the AMPKα1/ULK1/FUNDC1/mitophagy pathway. Redox Biol 52: 102288, 2022.
13. Lu D, Liu R, Zhou Y, Zhang Z, Jiang X, Xu J, Su A and Hu Z: FOXO3a-dependent up-regulation of HSP90 alleviates cisplatin-induced apoptosis by activating FUNDC1-mediated mitophagy in hypoxic osteosarcoma cells. Cell Signal 101: 110500, 2023.
14. Guo X, Zhang Z, Gu J, Ke P, Liu J, Meng Y, Zheng W, Que W, Fan R, Luo J, *et al*: FUDNC1-dependent mitophagy ameliorate motor neuron death in an amyotrophic lateral sclerosis mouse model. Neurobiol Dis 197: 106534, 2024.
15. Ansari A, Rahman MS, Saha SK, Saikot FK, Deep A and Kim KH: Function of the SIRT 3 mitochondrial deacetylase in cellular physiology, cancer, and neurodegenerative disease. Aging Cell 16: 4-16, 2017.
16. Bugga P, Alam MJ, Kumar R, Pal S, Chattopadyay N and Banerjee SK: Sirt3 ameliorates mitochondrial dysfunction andoxidative stress through regulating mitochondrial biogenesis and dynamics in cardiomyoblast. Cell Signal 94: 110309, 2022.
17. Sánchez A, Calpena AC and Clares B: Evaluating the oxidative stress in inflammation: Role of melatonin. Int J Mol Sci 16: 16981-17004, 2015.
18. Li H, Liu M and Zhang C: Women with polycystic ovary syndrome (PCOS) have reduced melatonin concentrations in their follicles and have mild sleep disturbances. BMC Womens Health 22: 79, 2022.
19. Liu L, Chen H, Jin J, Tang Z, Yin P, Zhong D and Li G: Melatonin ameliorates cerebral ischemia/reperfusion injury through SIRT3 activation. Life Sci 239: 117036, 2019.
20. Wu J, Yang Y, Gao Y, Wang Z and Ma J: Melatonin attenuates anoxia/reoxygenation injury by inhibiting excessive mitophagy through the MT2/SIRT3/FoxO3a signaling pathway in H9c2 cells. Drug Des Devel Ther 14: 2047-2060, 2020.
21. Rotterdam ESHRE/ASRM-Sponsored PCOS Consensus Workshop Group: Revised 2003 consensus on diagnostic criteria and long-term health risks related to polycystic ovary syndrome. Fertil Steril 81: 19-25, 2004.
22. Ji R, Jia FY, Chen X, Wang ZH, Jin WY and Yang J: Salidroside alleviates oxidative stress and apoptosis via AMPK/Nrf2 pathway in DHT-induced human granulosa cell line KGN. Arch Biochem Biophys 715: 109094, 2022.
23. Zhang J, Huang H, Xiao M, Jiang X, Yang Y, Huang M, Wang S, Zhu B and Zhao M: Erchen decoction ameliorates the rat model of polycystic ovary syndrome by regulating the steroid biosynthesis pathway. Phytomedicine 143: 156852, 2025.
24. Yi S, Zheng B, Zhu Y, Cai Y, Sun H and Zhou J: Melatonin ameliorates excessive PINK1/Parkin-mediated mitophagy by enhancing SIRT1 expression in granulosa cells of PCOS. Am J Physiol Endocrinol Metab 319: E91-E101, 2020.
25. Liu Z, Wang RH and Wang KH: Formononetin ameliorates polycystic ovary syndrome through suppressing NLRP3 inflammasome. Mol Med 31: 27, 2025.
26. Liu M, Xuan A, Zheng L, Li D, Chen C, Liu H, Lu G, Cheng Z, Zou Y, Zhi S, *et al*: Novel coumarin derivative SZC-6 as an allosteric activator of SIRT3 alleviates diabetic kidney disease via the SIRT3-Foxo3a signaling axis. Free Radic Biol Med 240: 29-45, 2025.
27. Fiorentino G, Cimadomo D, Innocenti F, Soscia D, Vaiarelli A, Ubaldi FM, Gennarelli G, Garagna S, Rienzi L and Zuccotti M: Biomechanical forces and signals operating in the ovary during folliculogenesis and their dysregulation: Implications for fertility. Hum Reprod Update 29: 1-23, 2023.
28. Xie C, Lu H, Zhang X, An Z, Chen T, Yu W, Wang S, Shang D and Wang X: Mitochondrial abnormality in ovarian granulosa cells of patients with polycystic ovary syndrome. Mol Med Rep 29: 27, 2024.
29. Zhang Q, Ren J, Wang F, Pan M, Cui L, Li M and Qu F: Mitochondrial and glucose metabolic dysfunctions in granulosa cells induce impaired oocytes of polycystic ovary syndrome through Sirtuin 3. Free Radic Biol Med 187: 1-16, 2022.
30. Srinivasan S, Guha M, Kashina A and Avadhani NG: Mitochondrial dysfunction and mitochondrial dynamics-The cancer connection. Biochim Biophys Acta Bioenerg 1858: 602-614, 2017.
31. Tilokani L, Nagashima S, Paupe V and Prudent J: Mitochondrial dynamics: Overview of molecular mechanisms. Essays Biochem 62: 341-360, 2018.
32. Che L, Wu JS, Du ZB, He YQ, Yang L, Lin JX, Lei Z, Chen XX, Guo DB, Li WG, *et al*: Targeting mitochondrial COX-2 enhances chemosensitivity via Drp1-dependent remodeling of mitochondrial dynamics in hepatocellular carcinoma. Cancers (Basel) 14: 821, 2022.
33. Mao R, He S, Lan J and Zhu WZ: Honokiol ameliorates cisplatin-induced acute kidney injury via inhibition of mitochondrial fission. Br J Pharmacol 179: 3886-3904, 2022.
34. Morigi M, Perico L, Rota C, Longaretti L, Conti S, Rottoli D, Novelli R, Remuzzi G and Benigni A: Sirtuin 3-dependent mitochondrial dynamic improvements protect against acute kidney injury. J Clin Invest 125: 715-726, 2015.
35. Wang Y, Ge Y, Hua S, Shen C, Cai B and Zhao H: Aloe-Emodin improves mitophagy in Alzheimer's disease via activating the AMPK/PGC-1α/SIRT3 signaling pathway. CNS Neurosci Ther 31: e70346, 2025.
36. Han X, Peng M, Wang X, Hu Y, Li G, Song Y, Lv Y and Chen N: Role of the AMPK/PGC-1α/SIRT3-Mediated mitochondrial dysfunction in the neurotoxicity of methanol. Mol Neurobiol 63: 134, 2025.
37. Megha KB, Arathi A, Shikha S, Alka R, Ramya P and Mohanan PV: Significance of melatonin in the regulation of circadian rhythms and disease management. Mol Neurobiol 61: 5541-5571, 2024.
38. Alizadeh M, Karandish M, Asghari Jafarabadi M, Heidari L, Nikbakht R, Babaahmadi Rezaei H and Mousavi R: Metabolic and hormonal effects of melatonin and/or magnesium supplementation in women with polycystic ovary syndrome: A randomized, double-blind, placebo-controlled trial. Nutr Metab (Lond) 18: 57, 2021.
39. Wang X, Meng K, He Y, Wang H, Zhang Y and Quan F: Melatonin stimulates STAR expression and progesterone production via activation of the PI3K/AKT pathway in bovine theca cells. Int J Biol Sci 15: 404-415, 2019.
40. Shao X, Yang Y, Liu Y, Wang Y, Zhao Y, Yu X, Liu J, Li YX and Wang YL. Orchestrated feedback regulation between melatonin and sex hormones involving GPER1-PKA-CREB signaling in the placenta. J Pineal Res 75: e12913, 2023.
41. Reiter RJ, Sharma RN, Manucha W, Rosales-Corral S, Almieda Chuffa LG, Loh D, Luchetti F, Balduini W and Govitrapong P: Dysfunctional mitochondria in age-related neurodegeneration: Utility of melatonin as an antioxidant treatment. Ageing Res Rev 101: 102480, 2024.
42. Zhang C, Suo M, Liu L, Qi Y, Zhang C, Xie L, Zheng X, Ma C, Li J, Yang J and Bu P: Melatonin alleviates Contrast-Induced acute kidney injury by activation of Sirt3. Oxid Med Cell Longev 2021: 6668887, 2021.
43. Xu S, Li L, Wu J, Fang H, Han Y, Huang Q, Chen Z and Zeng Z: Melatonin attenuates Sepsis-induced small-intestine injury by upregulating SIRT3-mediated oxidative-stress inhibition, mitochondrial protection, and autophagy induction. Front Immunol 12: 625627, 2021.